Experimental Neurology 321 (2019) 113028

Contents lists available at ScienceDirect

Experimental Neurology

journal homepage: www.elsevier.com/locate/yexnr

Research paper

Botch protects neurons from ischemic insult by antagonizing Notch-mediated neuroinflammation

Hao Li[a,1], Junwei Ma[b,1], Qi Fang[a], Haiying Li[c], Haitao Shen[c], Xiang Li[c], Qun Xue[a,*], Juehua Zhu[a,*], Gang Chen[c]

[a] Department of Neurology, The First Affiliated Hospital of Soochow University, 188 Shizi Street, Suzhou, 215006, Jiangsu Province, China
[b] Department of Neurosurgery, The Affiliated Hospital of Qingdao University, 16 Jiangsu Road, Qingdao, 266003, Shandong Province, China
[c] Department of Neurosurgery & Brain and Nerve Research Laboratory, The First Affiliated Hospital of Soochow University, 188 Shizi Street, Suzhou 215006, Jiangsu Province, China

ARTICLE INFO

Keywords:
Botch
Notch1
Neuronal cell death
Neuroinflammation
Neuroprotection

ABSTRACT

Owing to the continued high morbidity and high mortality rate after stroke, it is important to seek treatments other than conventional thrombolysis. Notch1 up-regulation participates in inflammatory responses after cerebral ischemia-reperfusion (I/R) injury, and it has been reported that Botch binds to and blocks Notch1 maturation. In this study, we investigated the role of Botch during cerebral (I/R) injury and explored its potential mechanisms. A middle-cerebral-artery occlusion/reperfusion (MCAO/R) model was established in adult male Sprague-Dawley rats in vivo, and cultured neurons and microglia were exposed to oxygen-glucose deprivation/reoxygenation (OGD/R) to mimic I/R injury in vitro. The results showed that protein levels of Botch and the Notch1 intracellular domain (NICD) were increased after MCAO/R. Furthermore, after overexpression of Botch, the generation of the activated form of Notch1, NICD, was decreased, while Botch knockdown or mutation led to an increase in NICD generation. As a result, Botch overexpression exhibited neuroprotective effects by significantly decreasing neurobehavioral phenotypes, improving infiltration of activated microglia, ameliorating inflammatory cytokine release, and inhibiting neuronal cell death. Conversely, Botch knockdown and mutation induced opposite effects. In addition, NICD was found to translocate to the mitochondria after OGD/R in neurons and microglia, which stimulated accumulation of reactive oxygen species in mitochondria and resulted in neuronal cell death and microglial activation. Botch overexpression inhibited the generation of NICD and decreased the translocation of NICD to the mitochondria, which inhibited neuronal cell death and ameliorated neuroinflammation. In conclusion, we found that Botch exerts neuroprotective effects via antagonizing the maturation of Notch1-induced neuronal injury and neuroinflammation, which may provide insights into novel therapeutic targets for the treatment of I/R injury.

1. Introduction

Stroke is among the top-leading causes of death and disability, which accounting for almost 5% of all disability-adjusted life-years and 10% of all death worldwide (Collaborators et al., 2018). Brain injury and neuronal death following focal cerebral ischemia develop from a series of pathological processes such as excitotoxicity, inflammation and apoptosis (Dirnagl et al., 1999). Intravenous thrombolysis and mechanical thrombectomy are approved therapies for the acute treatment of stroke (Powers et al., 2018). However, no neuroprotective therapy has been efficacious (Stocchetti et al., 2015). Thus, it is of great value to explore innovative neuroprotective strategies for treating stroke.

Botch (also known as CHAC1) is a novel endogenous Notch inhibitor that inhibits the S1 furin-like cleavage of Notch1 (Chi et al., 2014; Li et al., 2012a). Our previous study demonstrated that Notch1-Dll4

Abbreviations: DAPT, [N-(3,5-difluorophenacetyl)-1-alanyl]-*S*-phenylglycine t-butyl ester; I/R injury, ischemia/reperfusion (I/R) injury; MCAO/R, middle cerebral artery occlusion/ reperfusion; MCA, middle cerebral artery; TTC, 2, 3, 5-triphenyltetrazolium chloride; siRNA, small interfering RNA; AAV, adeno-associated virus; OGD/R, oxygen-glucose deprivation/reoxygenation; TNF-α, tumor necrosis factor-α; IL-6, interleukin-6; PBS, phosphate buffer saline; FJB, Fluoro-Jade B; NICD, Notch intracellular domain; ROS, reactive oxygen species

* Corresponding authors at: Department of Neurology, The First Affiliated Hospital of Soochow University, 188 Shizi Street, Suzhou 215006, China.
E-mail addresses: qxue_sz@163.com (Q. Xue), zhujuehua0216@suda.edu.cn (J. Zhu).

[1] These authors contributed equally to this work.

https://doi.org/10.1016/j.expneurol.2019.113028
Received 4 April 2019; Received in revised form 27 July 2019; Accepted 31 July 2019
Available online 01 August 2019
0014-4886/

signaling is activated in the ischemic hemisphere (Zhu et al., 2015). Additionally, Notch signaling has been shown to exacerbate brain damage and the functional outcome in ischemic stroke (Arumugam et al., 2006). The gamma-secretase inhibitor, *N*-[*N*-(3,5-difluorophenacetyl)-1-alanyl]-*S*-phenylglycine t-butyl ester (DAPT), suppresses the activation of Notch1. Evidence has been provided that DAPT alleviates neuronal death and decreases the infarction volume after stroke (Li et al., 2012b; Li et al., 2016a). One study has demonstrated that Botch protects neurons in hemorrhagic stroke (Mei et al., 2017). However, no studies have been conducted on the pathogenic role of Botch in ischemia/reperfusion (I/R) injury during ischemic stroke.

The aim of the current study was to investigate the role of Botch in ischemic stroke and its impact on neuroinflammation following ischemic injury. A better understanding of Botch functionalities and mechanisms during ischemic stroke may provide insights into novel therapeutic targets for the treatment of I/R injury.

2. Materials and methods

2.1. Animals

Male Sprague-Dawley (SD) rats (250–300 g) were purchased from the Animal Center of Chinese Academy of Sciences (Shanghai, China). All rats were allowed free access to food and water under controlled conditions (12/12 h light/dark cycle with humidity of 60% ± 5%, 22 ± 3 °C). Additionally, primary neuronal and microglial cultures in vitro were prepared using 16–18-day-old pregnant SD rats. All the experimental protocols were approved by the Ethics Committee of the First Affiliated Hospital of Soochow University and its institutional animal-care committee. The animal experiments complied with the ARRIVE guidelines and were carried out in strict accordance with the National Institutes of Health guide for the care and use of laboratory animals (NIH Publications No. 8023, revised 2011). All efforts were made to minimize the number of animals sacrificed and any suffering during the study.

2.2. Rat model of middle-cerebral-artery occlusion/reperfusion

Focal cerebral ischemia was induced by right-intraluminal middle-cerebral-artery (MCA) occlusion, as described previously (Zhu et al., 2015). Briefly, after rats were anesthetized with 4% chloral hydrate (10 ml/kg i.p.), a 6-0 silicone-coated nylon filament with a heat-rounded tip that was coated with 0.01% poly-L-lysine was advanced from the external carotid artery into the lumen of the internal carotid artery until the rounded tip reached the entrance to the MCA. The decline of blood flow in the MCA supply territory was confirmed by a laser Doppler flowmeter (LDF; Perimed PF5000, Stockholm, Sweden). Rats that presented at least a 70% decrease of the baseline blood flow were included in the following experiments. The rats were then briefly re-anesthetized, and the filament was withdrawn to restore the blood flow 120 min after occlusion. Body temperature was maintained at 36.5–37.5 °C using a heating pad during the procedure. In the sham group, all the procedures were the same as those for the stroked groups, except that the filament was inserted less deeply so that it would not block the blood flow in the MCA supplied area. Infarction caused by 2 h of MCAO/R is shown in Fig. 1A by 2, 3, 5-triphenyltetrazolium chloride (TTC) staining.

2.3. Cell culture

Primary rat cortical neurons and microglia were obtained and cultured as described previously (Shen et al., 2017). Briefly, cortical neurons were prepared from embryonic-day-19 at brains. Then, cortical neurons were digested with 0.25% trypsin-EDTA solution for 5 min at 37 °C. The dissociated neurons were seeded on 150 cm^2 culture flasks (Corning, USA) precoated with poly-D-lysine (Sigma, USA), and were cultured in neurobasal medium containing 2% B-27, 0.5 mM of GlutaMAX, 50 U/ml of penicillin, and 50 U/ml of streptomycin (all from Invitrogen, Grand Island, NY, USA) under humidified air containing 5% CO_2 at 37 °C. Similarly, primary rat cortical microglia were obtained from one-day-old rats and were cultured in DMEM/F12 medium (containing 10% fetal bovine serum, 1 mM sodium pyruvate, 2 mM L-glutamine, 100 mM non-essential amino acids, 50 U/ml penicillin and 50 U/ml streptomycin). Half of the culture medium was replaced with fresh medium every two days.

2.4. Experimental design

To verify the expression pattern of Botch after ischemic attack (experiment 1; Fig. 1B), rats under sham ($N = 6$) or MCAO/R ($N = 50$, 42 survived) surgeries were included. Animals experiencing MCAO/R were sacrificed at different intervals (1, 3, 6, 12, 24, 48, or 72 h after MCAO/R). Additionally, brains tissue samples were obtained for analysis. To investigate neuroprotection of Botch after ischemic injury in vivo (experiment 2; Fig. 1C), specific small-interfering RNA (siRNA) against Botch was applied to knockdown Botch, and adeno-associated viral (AAV) vectors were used to overexpress Botch. Rats were divided into the following six groups: sham group (sham), MCAO/R group, MCAO/R + Si-negative control group (CtrSiRNA), MCAO/R + SiRNA-Botch group (SiRNA), MCAO/R + vector group (Vector), and MCAO/R + Botch-overexpression group (Over-Botch). The MCAO/R surgery was performed 48 h after the transfection of siRNA or two weeks after the transfection of AAV in vivo. At 24 h after MCAO/R, rats were sacrificed and the brain samples were collected for analysis. Rats in the neurobehavior groups were tested at 0-, 1-, 3-, 7-, and 14-day intervals after MCAO/R. To confirm the neuroprotection of Botch and its possible mechanism (experiments 3 and 4; Fig. 1D–E), the following in vitro studies were conducted. Based on the interventions 48 h before oxygen and oxygen-glucose deprivation/reoxygenation (OGD/R), the primary cultured neurons or microglia were divided into the following six groups: normal group (Normal), OGD/R group, OGD/R + Si-negative control group (CtrSiRNA), OGD/R + SiRNA-Botch group (SiRNA), OGD/R + vector group (Vector), and OGD/R + Botch-WT group (Over-Botch). At 12 h after OGD/R, cells were used for testing. Living cells were used for the MitoSox test.

2.5. Antibodies

The following antibodies were purchased from Abcam: Rb pAb for the CHAC 1 antibody (ab 76,386), Rb pAb for labeling activated Notch1 (ab 52,301), Ms. mAb for the HA tag (ab 18,181), Ms. mAb for labeling GFP (ab 1218), Rb mAb for labeling NeuN (ab 177,487), Ms. mAb for labeling NeuN (ab 104,224), and Ms. mAb for labeling Iba1 (ab 15,690). A cleaved Notch Rabbit mAb (va11744) was purchased from Cell Signaling Technology. Secondary antibodies for western blot analysis, including anti-rabbit IgG-HRP (7074 s) and anti-mouse IgG-HRP (7076 s), were purchased from Cell Signaling Technology. Secondary antibodies for immunofluorescence were purchased from Life Technologies and included the following: Alexa Fluor-488 donkey anti-rabbit IgG antibody (A21206), Alexa Fluor-488 donkey anti-mouse IgG antibody (A21202), Alexa Fluor-555 donkey anti-mouse IgG antibody (A31570), and Alexa Fluor-555 donkey anti-rabbit IgG antibody (A31572).

2.6. Construction of siRNAs and botch overexpression system

A specific siRNA against Botch was obtained from Ribobio (Ribobio Co., LTD, Guangzhou, China) to knockdown Botch expression. The three different Botch-target sequences used in this study were as follows: GAGAGAAGCTGTGCTTGGT, CACTGAAGTACCTGAACGT, and CTAAGGAAGTCACCTTTTA. The efficiencies of all three siRNAs to knockdown Botch expression were tested, and the most efficient siRNA

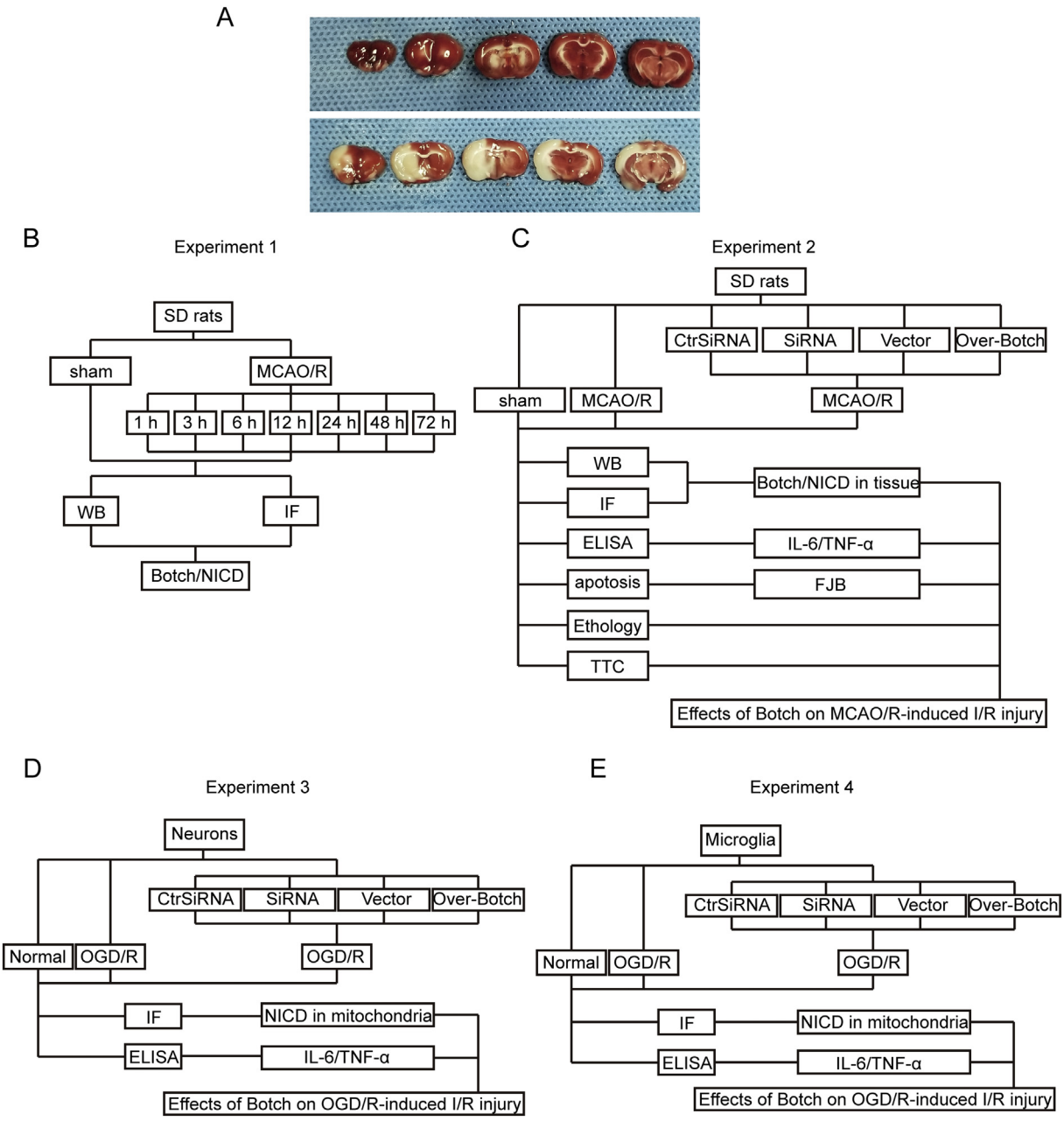

Fig. 1. Establishment of the MCAO/R model and experimental design.
(A) Brain slices from sham and MCAO/R-injured rats. (B) Experimental design displaying the change of Botch and NICD proteins at different time points after MCAO/R. (C) Effects of Botch on MCAO/R-induced I/R injury in rats after the indicated interventions. (D) Effects of Botch on Notch activation and NICD mitochondria translocation after OGD/R in neurons. (E) Effects of Botch on NICD translocation and ROS production, as well as microglia-secreted pro-inflammatory cytokines after OGD/R in microglia.

was used in this study.

Specific over-expression plasmids for Botch were obtained from the Dawson lab (Institute for Cell Engineering, Johns Hopkins University School of Medicine). Specifically, the target fragment was sub-cloned into a pZC18 expression vector to produce the PZC18-Botch plasmid. All of the constructs were tested by DNA sequencing. Then, the target fragment was sub-cloned into a HBAAV2/9-CMV expression vector to produce the HBAAV2/9-CMV-r-Botch-HA-GFP plasmid. Next, this plasmid was applied in vitro for Botch overexpression in cultured cells. For in vivo Botch-overexpression experiments, the above plasmid was packaged into an AAV vector (Hanbio Biotechnology Co. Ltd.) and its titer was determined. The titer of the AAV was 1×10^{12} vg/ml.

2.7. Transfection of siRNA or AAV in vivo

To transfect siRNA, Entranster in vivo RNA transfection reagent (18668–11-1 Engreen) was used per the manufacturer's instructions. The procedure of intracerebroventricular injection of siRNA or AAV was performed as described previously (Li et al., 2018). Briefly, the injection site selected was in the right hemisphere at 1.0 mm lateral to the midline and 1.5 mm posterior to bregma. The needle of the microinjector was slowly inserted into the lateral ventricle at 3.5 mm below the dural surface. Ten μl of siRNA or 5 μl of AAV was infused in at a rate of approximately 5 μl /min.

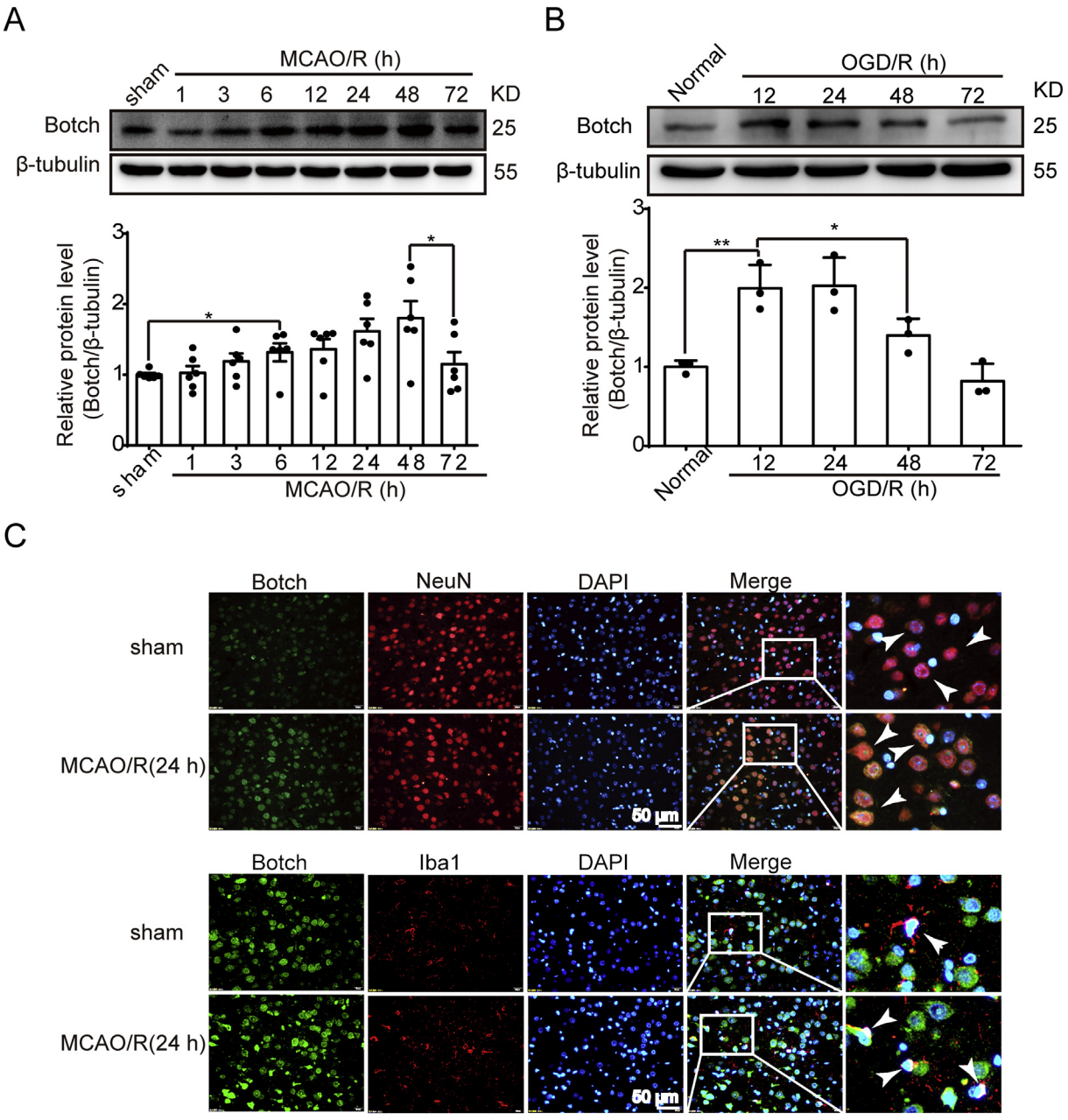

Fig. 2. Botch expression increases after ischemic insult.
(A) Western blot analysis and quantification of the protein levels of Botch in brain tissue around the ischemic penumbra. (B) Western blot analysis and quantification of the protein levels of Botch in cultured neurons. (C) Double-immunofluorescence analysis was performed with Botch antibodies (green), a neuronal marker (NeuN, red) or microglia marker (Iba1, red), and nuclei were fluorescently labeled with DAPI (blue). Arrows point to Botch-positive neurons or microglia (scale bar = 50 μm). In (A–B), mean values for sham group were normalized to 1.0. (A) 6 h vs. sham, $*p < .05$; 12 h vs. sham, $*p < .05$; 24 h vs. sham, $**p < .01$; 48 h vs. sham, $**p < .01$; 48 h vs. 72 h, $*p < .05$. (B) 12 h vs. normal, $**p < .01$; 24 h vs. Normal, $**p < .01$; 12 h vs. 48 h, $*p < .05$. (For interpretation of the references to colour in this figure legend, the reader is referred to the web version of this article.)

2.8. Transfection of plasmid and siRNA in cultured cells

Cultured neurons or microglia were transfected with the indicated expression plasmid using Lipofectamine® 3000 Transfection Reagent (Invitrogen, L3000-015) or siRNAs using Lipofectamine RNAi MAX (Invitrogen, 13,778-075), according to the manufacturer's instructions. At 48 h after transfection, neurons or microglia were treated with OGD/R. Twelve hours later cells were harvested for further analysis.

2.9. Western blot analysis

Western blot analysis was performed as described previously (Wang et al., 2016; Yuan et al., 2016). Briefly, the brains tissue samples or extracted cells were mechanically lysed in ice-cold RIPA lysis buffer (Beyotime, Shanghai, China). After centrifugation at 12,000 RPM for 15 min at 4 °C, the supernatants were collected. Then we used an enhanced BCA Protein Assay Kit (Beyotime, Shanghai, China) to measure protein concentrations by the bicinchoninic-acid method. The protein samples (50 μg/lane) were loaded onto a 10% SDS-polyacrylamide gel and were separated and electrophoretically transferred to a nitrocellulose membrane (Millipore Corporation, Billerica, MA, USA), which was blocked with 5% non-fat milk for 2 h at room temperature. Then, the membrane was incubated with primary antibody overnight at 4 °C. The titers of antibodies use in immunoblots were as follows: Rb

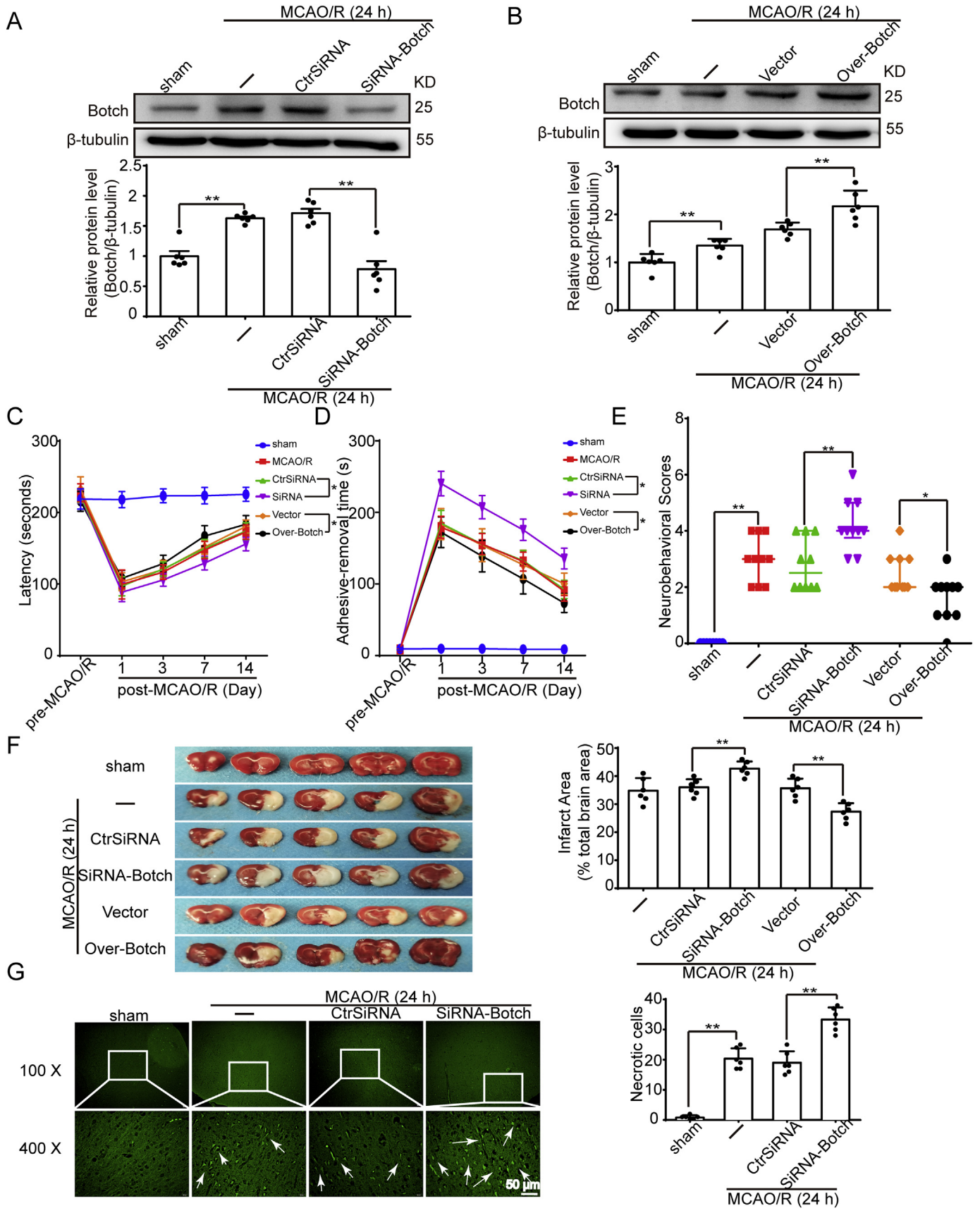

(caption on next page)

Fig. 3. Botch exerts neuroprotection in rat MCAO/R.
(A, B) Transfection efficiency of Botch adenovirus associated virus (AAV) and siRNA in rat brains. (C) Rotarod test. (D) Adhesive-removal test. (E) Neurological behavioral scores. (F) Triphenyltetrazolium chloride (TTC) staining and (G) FJB staining showing the effects of Botch intervention on neuronal necrosis. Arrows point to FJB-positive cells in the brain (scale bar = 50 μm). Quantification of the FJB staining as shown. In (A-B), mean values for sham group were normalized to 1.0. (A) 24 h vs. sham, $^{**}p < .01$; CtrSiRNA vs. sham, $^{**}p < .01$; CtrSiRNA vs. SiRNA-Botch, $^{**}p < .01$. (B) 24 h vs. sham, $^{**}p < .01$; Vector vs. sham, $^{**}p < .01$; Over-Botch vs. sham, $^{**}p < .01$; Vector vs. Over-Botch, $^{**}p < .01$. (C) CtrSiRNA vs. SiRNA, $^{*}p < .05$, Vector vs. Over-Botch, $^{*}p < .05$. (D) CtrSiRNA vs. SiRNA, $^{*}p < .05$, Vector vs. Over-Botch, $^{*}p < .05$. (E) CtrSiRNA vs. SiRNA, $^{**}p < .01$, Vector vs. Over-Botch, $^{*}p < .05$. (F) CtrSiRNA vs. SiRNA, $^{**}p < .01$, Vector vs. Over-Botch, $^{**}p < .01$. (G) sham vs. MCAO/R (24 h), $^{**}p < .01$, CtrSiRNA vs. SiRNA, $^{**}p < .01$.

pAb to CHAC 1 antibody (Abcam, ab 76,386, 1:1000 dilution), Rb pAb to activated Notch1 (ab 52,301, 1:1000 dilution), Ms. mAb to GFP (ab1218, 1:1000 dilution), cleaved Notch Rabbit mAb (Cell Signaling Technology, va11744, 1:500 dilution). Additionally, β-tubulin was detected as a loading control. Then, the membranes were probed with corresponding HRP-conjugated secondary antibodies for 2 h at room temperature. Finally, we revealed the band signals via an Enhanced Chemiluminescence (ECL) Kit. The relative quantities of proteins were analyzed using Image J (NIH, Bethesda, MD, USA) and were normalized to that of the loading control.

2.10. Immunofluorescent analysis

The brain tissue samples were fixed in 4% paraformaldehyde, embedded in paraffin, cut into 4 μm sections. Similarly, the cultured cells were fixed with 4%paraformaldehyde. Then, the sections and cells were probed with primary antibodies and appropriate secondary antibodies. The titers of antibodies use in immunofluorescence were as follows: Rb pAb to CHAC 1 antibody (Abcam, ab 76,386, 1:200 dilution), Rb mAb to NeuN (ab 177,487, 1:200 dilution), Ms. mAb to NeuN (ab 104,224, 1:200 dilution), Ms. mAb to Iba1 (ab 15,690, 1:200 dilution), cleaved Notch Rabbit mAb (Cell Signaling Technology, va11744, 1:100 dilution). Normal rabbit IgG, normal mouse IgG, and normal goat IgG were used as negative controls for the immunofluorescence assay. Nuclei were stained with DAPI mounting medium. Finally, the sections and cells were observed by a fluorescence microscope (OLYMPUS BX50/BX-FLA/DP70; Olympus Co., Tokyo, Japan) or laser scanning confocal microscope (ZEISS LSM 880, Carl Zeiss AG, Germany).

2.11. Fluoro-Jade B (FJB) staining

Cell necrosis in brain tissue was detected by FJB staining. Brain sections were deparaffinized and dehydrated. The slides were subsequently transferred to a solution of 0.06% potassium permanganate for 15 min and were gently shaken on a rotating platform. Then, the slides were rinsed in deionized water and immersed in FJB working solution (0.001% FJ/0.1% acetic acid) for 20 min. The brain sections were subsequently rinsed three times (1 min each) with distilled water and were dried in an incubator (50–60 °C) for 10 min. Finally, sections were cleared in xylene and cover slipped with a non-aqueous, low-fluorescence, styrene-based mounting medium (DPX, Sigma-Aldrich, MO, U.S.). The sections were visualized by a fluorescent microscope (OLYMPUS BX50/BX-FLA/DP70; Olympus Co., Tokyo, Japan). The number of FJB positive cells in each section was calculated carefully per sample, and cell counts from the section were averaged to provide the mean value.

2.12. Estimation of infarct volume by TTC staining

Following the MCAO/R procedure, rats were euthanized at 24 h after reperfusion. The forebrains were dissected into 2-mm coronal slices. The slices were incubated with 2% solution of TTC (Nanjing Jiancheng Bioengineering Institute, Nanjing) in phosphate buffer saline (PBS) at 37 °C for 30 min. The infarcted tissue was verified by the complete loss of TTC staining, contrasting with the red-stained viable tissue. The area of infarction was determined by Image J software.

2.13. Behavioral tests

In all animals, a battery of behavioral tests was performed before MCAO/R and at 1, 3, 7 and 14 days after MCAO/R by two investigators who were blind to the experimental design.

2.14. Neurological scoring

At 72 h after MCAO/R, neurological tests were conducted on 12 rats per group to assess behavioral impairments. Behavioral performance was scored according to a previously published scoring system that monitored appetite, activity, and neurologic defects (Wang et al., 2015).

2.15. Rotarod test

An accelerating rotarod test was employed to measure the motor function of rats (Chen et al., 2001; Zhang et al., 2000). The diameter of the rotarod spindle was 10 cm. The speed of the spindle was increased from 4 to 30 rpm in 60 s and 30 rpm was maintained for a maximum of 300 s. When the rats lost their balance and fell off the rotarod, it triggered the sensor and the time was recorded. Through separation by two panels to prevent the rats from detecting each other, three rats were able to run simultaneously. Before testing, each rat received three training sessions per day for three consecutive days and the last three records were counted as the baseline. Then, all rats received a test trial on an accelerating rotarod at all testing days after MCAO/R.

2.16. Adhesive-removal test

The adhesive removal test was performed as described previously (Zhang et al., 2000). Briefly, the rats were removed from their home cage and trained to be familiar with the testing environment. Then, two small pieces of adhesive-backed paper dots were glued to the wrist of each forelimb. The rats were then gently returned to their testing cages. The time required to remove both stimuli from each limb was recorded in five trials per day for three days. If the rats were able to remove the dots within 10 s at the end of training, then the rats were included in the experimental group. Then, all rats received a test trial at all testing days after MCAO/R.

2.17. Assay of inflammatory cytokines (tumor necrosis factor α and interleukin 6)

We used a specific rat tumor necrosis factor α (TNF-α) ELISA Kit (Bio-Swamp, Wuhan, China) and a rat interleukin 6 (IL-6) ELISA Kit (Bio-Swamp, Wuhan, China) to quantify the levels of TNF-α and IL-6 in the serum and medium, according to the manufacturer's instructions.

2.18. MitoSox test

We used a stock solution of 5-mM MitoSOX reagent (Sigma-Aldrich, St. Louis, MO, USA). Specifically, the contents (50 μg) were dissolved into one vial of MitoSOX mitochondrial superoxide indicator (Component A) in 13 μl of dimethylsulfoxide (DMSO) to make the stock solution of 5-mM MitoSOX reagent. Then, we prepared a 5-μM MitoSOX

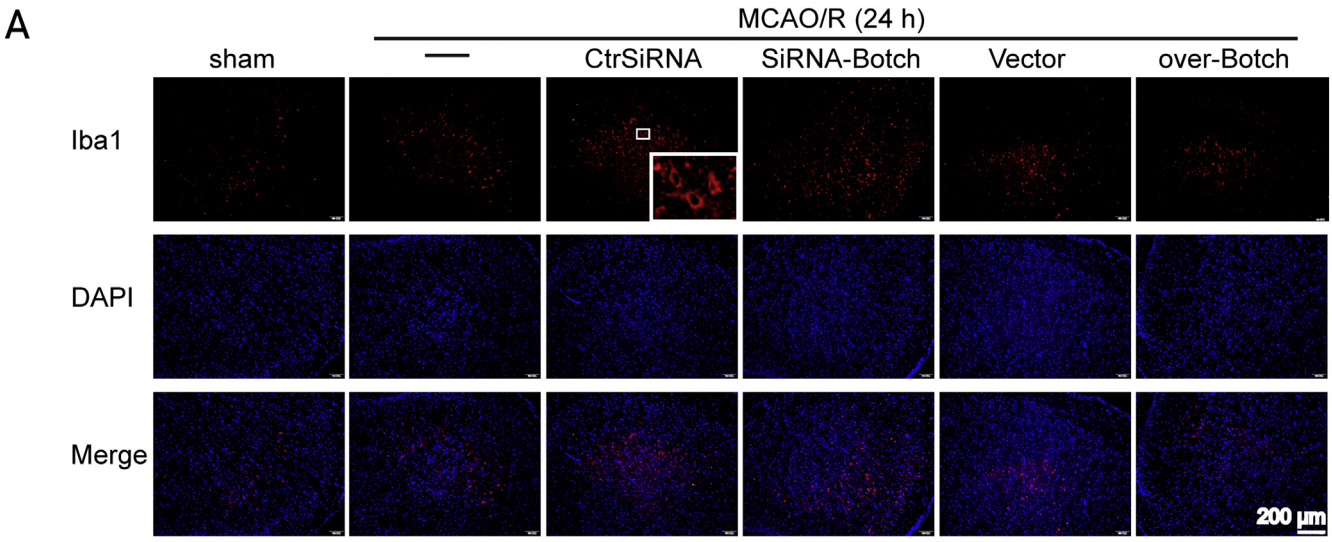

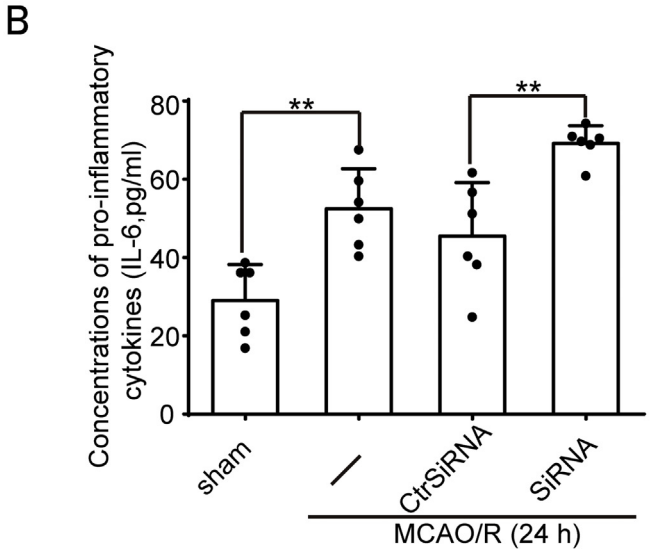

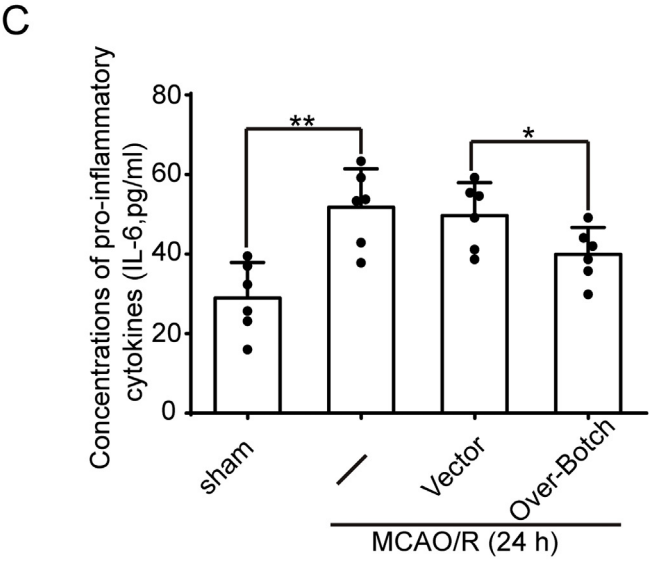

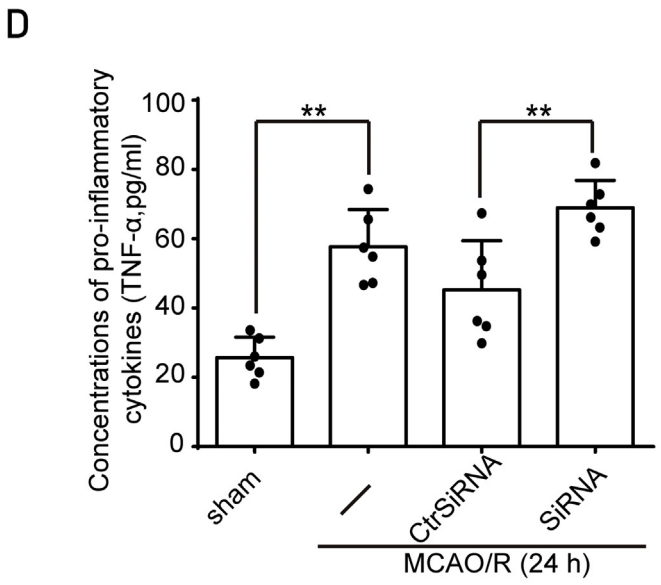

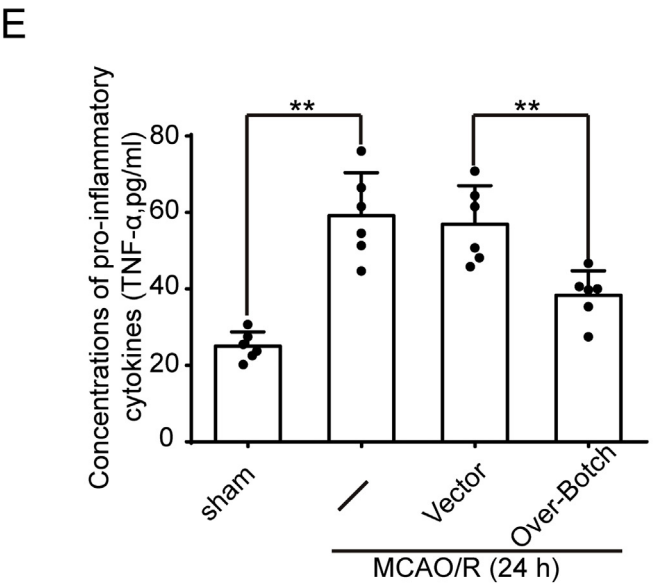

(caption on next page)

Fig. 4. Botch mediates microglial infiltration and neuroinflammation after MCAO/R.
(A) Immunofluorescent analysis was performed with a microglial marker (Iba1, red), and nuclei were fluorescently labeled with DAPI (blue). (B, C, D, E) Concentrations of pro-inflammatory cytokines (IL-6 and TNF-α) in the serum were assayed by ELISA. (B) 24 h vs. sham, **p < .01; CtrSiRNA vs. SiRNA, **p < .01. (C) 24 h vs. sham, **p < .01; Over-Botch vs. vector, *p < .05. (D) 24 h vs. sham, **p < .01, CtrSiRNA vs. SiRNA-Botch, **p < .01. (E) 24 h vs. sham, **p < .01; Over-Botch vs. vector, **p < .01. (For interpretation of the references to colour in this figure legend, the reader is referred to the web version of this article.)

reagent working solution. We then diluted the 5-mM MitoSOX™ reagent stock solution (prepared above) in PBS to make a 5-μM MitoSOX™ reagent working solution. We applied 1.0–2.0 ml of 5-μM MitoSOX™ reagent working solution to cover the neurons. The neurons were then incubated for 10 min at 37 °C and were protected from light. Subsequently, the neurons were gently washed three times with warm PBS. Neurons were stained with counterstains and were mounted in warm PBS for imaging and analysis.

2.19. Statistics

Statistical analyses were performed with Prism software version 6.0 (GraphPad). Data are presented as means ± SDs or medians with interquartile ranges (IQRs). Differences between groups were determined with two-tailed Student's *t*-tests or Mann-Whitney *U* tests for comparisons between two groups or by a one-way analysis of variance (ANOVA) followed by Tukey's post hoc tests for comparisons of more than two groups. Statistical significance was determined as $P < .05$ unless otherwise stated.

3. Results

3.1. Botch expression increases after ischemic injury

To explore the expression of Botch in brain tissue after MCAO/R, we detected the protein levels of Botch by western blotting in vivo (Fig. 2A) and in vitro (Fig. 2B). After MCAO/R modeling in rats, protein levels of Botch were significantly elevated at 6 h after MCAO/R and peaked at 48 h after MCAO/R (Fig. 2A). Immunostaining of brain tissue 24 h after MCAO/R demonstrated that Botch was expressed in $NeuN^+$ neurons and $Iba1^+$ microglia (Fig. 2C). In cultured primary neurons after OGD/R modeling, Botch expression was also significantly increased at 12 h and peaked by 12–24 h (Fig. 2B).

3.2. Botch exerts neuroprotection in a rat model of MCAO/R

To further identify the role of Botch in ischemic stroke, we adopted siRNA against Botch to decrease its expression and AAV packaged HBAAV2/9-CMV-r-Botch-HA-GFP to increase its expression before the initiation our rat model of MCAO/R. The interfering effects of siRNA and AAV-vector were confirmed by western blotting (Fig. 3A, B). Behavioral tests provided evidence that Botch improved neurological outcomes after ischemic stroke. Botch upregulation alleviated the sensory and motor deficits caused by MCAO/R, as suggested by results of the rotarod test (Fig. 3C), adhesive-removal test (Fig. 3D), and neurobehavioral scores (Fig. 3E), while Botch downregulation exacerbated the neurological dysfunction following ischemic stroke.

At the tissue level, showed by TTC staining, siRNA knockdown of Botch led to an enlarged ischemic volume after MCAO/R, while overexpression of Botch reduced the ischemic volume (Fig. 3F). At the cellular level, FJB staining confirmed that Botch knockdown increased neuronal death as compared with those of the siRNA-Botch and CtrSiRNA groups (Fig. 3G).

3.3. Botch alleviates microglial infiltration and neuroinflammation after MCAO/R

After ischemic stroke, microglia were activated ($Iba1^+$) and distributed in a cluster-like pattern (Fig. 4A). Upregulation of Botch reduced the number of activated microglia, and downregulation of Botch increased microglial activation (Fig. 4A). TNF-α and Il-6 are believed to be secreted by microglia and are important mediators of neuroinflammation in stroke. We found that, consistent with the activation pattern of microglia, upregulation of Botch reduced the expression levels of the pro-inflammatory cytokines, IL-6 and TNF-α, after MCAO/R, whereas downregulation of Botch led to higher levels of pro-inflammatory cytokines (Fig. 4B, C).

3.4. Botch antagonizes the activation of the Notch1 signaling pathway

Previous studies have revealed that Botch inhibits Notch signaling by preventing the S1 furin-like cleavage of Notch. Our in vivo and in vitro western blotting data showed that there was an increased expression of the Notch intracellular domain (NICD) after MCAO/R (Fig. 5A) and OGD/R (Fig. 5B). Knockdown of Botch upregulated the NICD protein level in rat brains after MCAO/R (Fig. 5C), while overexpression of Botch downregulated the NICD maturation (Fig. 5D). Similar results were found in in vitro OGD/R neurons when Botch was overexpressed using a plasmid expressing Botch-GFP, or blocked using siRNA-Botch (Fig. 5E, F).

3.5. Botch decreases neuroinflammation and accumulation of reactive oxygen species by inhibiting NICD translocation

As indicated by immunofluorescent staining, NICD was found to translocate to the mitochondria in neurons and microglia after OGD/R (Fig. 6A). The process of NICD translocation to mitochondria is believed to stimulate accumulation of reactive oxygen species (ROS) within mitochondria; the latter ultimately results in neuronal cell death and microglial activation (Jun et al., 2015). Using a fluorescent microplate reader, we confirmed that when Botch was overexpressed, the accumulation of oxidizing substances in neurons was significantly reduced; when Botch was knocked down, the accumulation of oxidizing substances increased (Fig. 6B, C). Consistently, after OGD/R injury in microglia, microglia with upregulated Botch had decreased expressions of the pro-inflammatory cytokines, IL-6 and TNF-α, whereas microglia with downregulated Botch had higher expression levels of pro-inflammatory cytokines (Fig. 6D, E).

4. Discussion

The current study provides evidence that Botch is a potential neuroprotective target. Botch ameliorated neurological dysfunction after ischemic stroke and reduced infarction volume, neuronal death and microglial activation. A potential mechanism by which Botch alleviated microglial neuroinflammation is that Botch may have blocked NICD injury-induced upregulation and mitochondrial translocation. Previous studies have shown that Botch promotes neurogenesis in mouse embryos (Chi et al., 2012a). In cerebrovascular disease, Botch has been demonstrated to inhibit Notch1-dependent neuroinflammation and,thereafter, alleviate early brain injury induced by subarachnoid hemorrhage (Liu et al., 2019). Botch also plays a neuroprotective role in the secondary brain injury of hemorrhagic stroke (Mei et al., 2017). Consistently, in this study, we elucidated a neuroprotective role of Botch in ischemic stroke, both in vitro and in vivo.

In the current study we confirm that in the condition of ischemic and prefusion injury, Botch activation inhibits the maturation of Notch, which is was presented by the formation of NICD. Animals with Botch

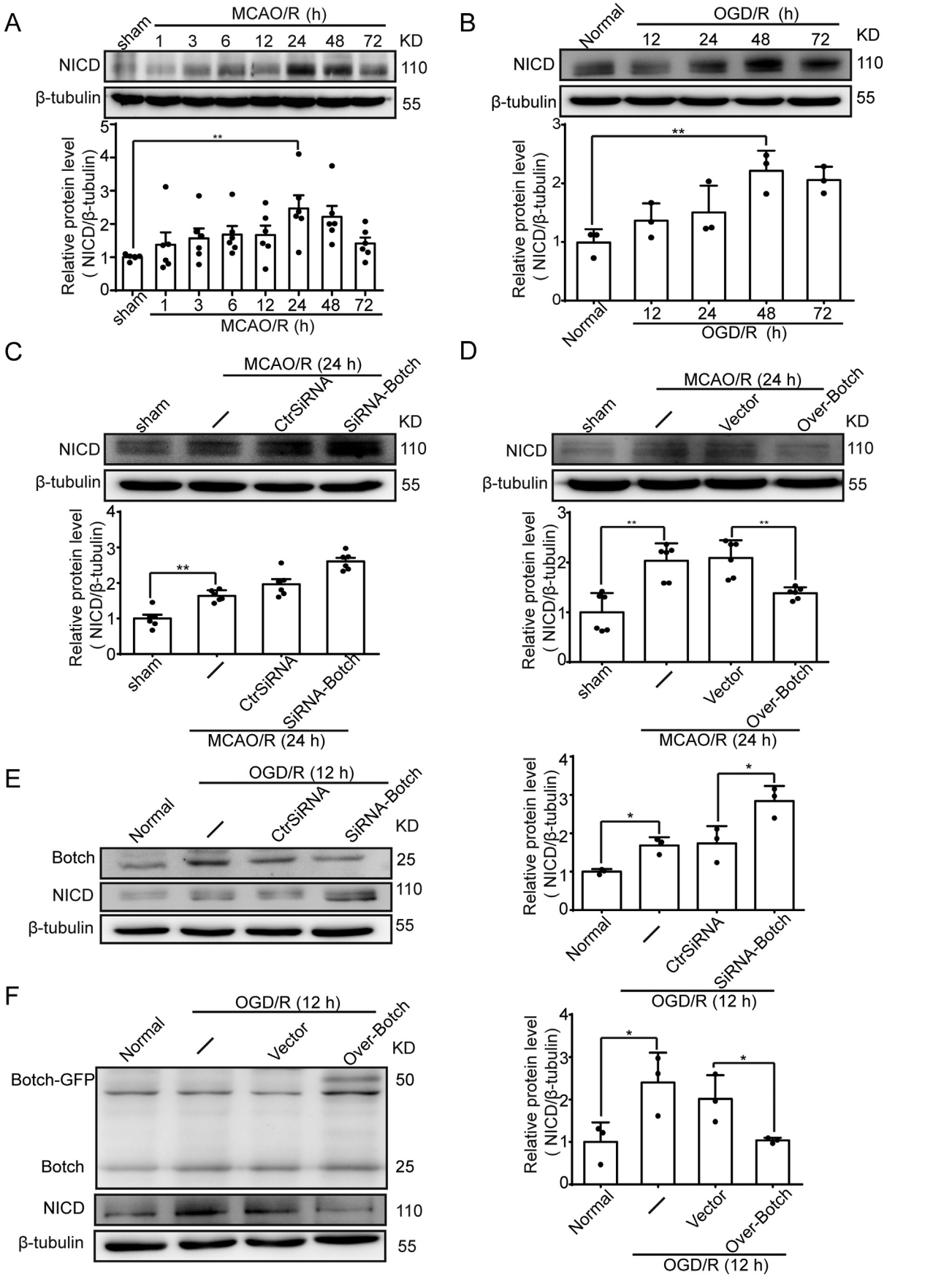

(caption on next page)

Fig. 5. Botch antagonizes the activation of the Notch1 signaling pathway.
(A) Western blot analysis and quantification of the protein levels of NICD in brain tissue around the ischemic penumbra. (B) Western blot analysis and quantification of the protein levels of NICD in cultured neurons. (C, D) Effects of overexpression and knockdown of Botch on the protein levels of NICD in brain tissue under ischemic MCAO/R. (E, F) Effects of overexpression and knockdown of Botch on the protein levels of NICD in cultured neurons under OGD/R. In (A–F), mean values for the sham group were normalized to 1.0. (A) 6 h vs. sham, *p < .05; 12 h vs. sham, *p < .05; 24 h vs. sham, **p < .01; 48 h vs. sham, **p < .01; 72 h vs. sham, *p < .05. (B) 48 h vs. Normal, **p < .01; 72 h vs. Normal, **p < .01. (C) 24 h vs. sham, **p < .01; CtrSiRNA h vs. sham, **p < .01; SiRNA-Botch vs. sham, **p < .01. (D)24 h vs. sham, **p < .01; Vector vs. sham, **p < .01; Over-Botch vs. sham, *p < .05; Vector vs. Over-Botch, **p < .01. (E) SiRNA-Botch vs. Normal, **p < .01; CtrSiRNA vs. SiRNA, *p < .05. (F)24 h vs. Normal, *p < .05; Vector vs. Over-Botch, *p < .05.

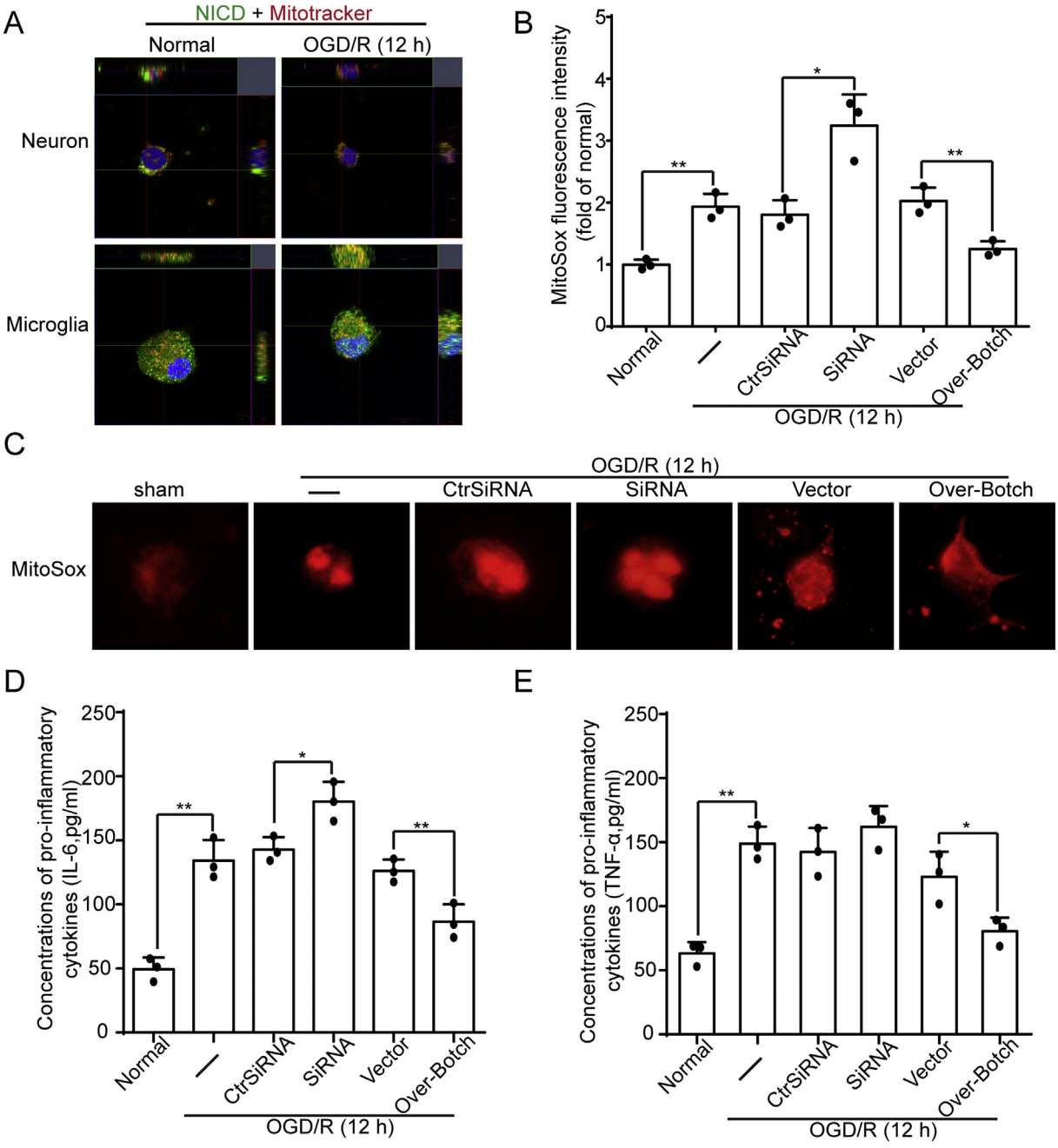

Fig. 6. Botch decreases neuroinflammation and ROS accumulation.
(A) Fluorescent confocal microscopy shows the colocalization of NICD (green) and MitoTracker (red) in neurons or microglial cells treated with I/R injury in vitro. Nuclei were fluorescently labeled with DAPI (blue). (B) Fluorescent microplate reader analysis of mtROS using MitoSox Red in neurons treated with OGD/R for 12 h. (C) Immunofluorescence analysis of mtROS using MitoSox Red in neurons treated with OGD/R for 12 h. (D, E) Concentrations of pro-inflammatory cytokines (IL-6 and TNF-α) in medium were assayed by ELISA. (B) 24 h vs. Normal, **p < .01; CtrSiRNA vs. Normal, **p < .01; SiRNA vs. Normal, **p < .01; Vector vs. Normal, **p < .01; Over-Botch vs. Normal, *p < .05; CtrSiRNA vs. SiRNA-Botch, *p < .05; Vector vs. Over-Botch, **p < .01. (D) 24 h vs. Normal, **p < .01; CtrSiRNA vs. Normal, **p < .01; SiRNA vs. Normal, **p < .01; Vector vs. Normal, **p < .01; Over-Botch vs. Normal, *p < .05; CtrSiRNA vs. SiRNA-Botch, *p < .05; Vector vs. Over-Botch, **p < .01. (E) 24 h vs. Normal, **p < .01; CtrSiRNA vs. Normal, **p < .01; SiRNA vs. Normal, **p < .01; Vector vs. Normal, **p < .01; Vector vs. Over-Botch, *p < .05. (For interpretation of the references to colour in this figure legend, the reader is referred to the web version of this article.)

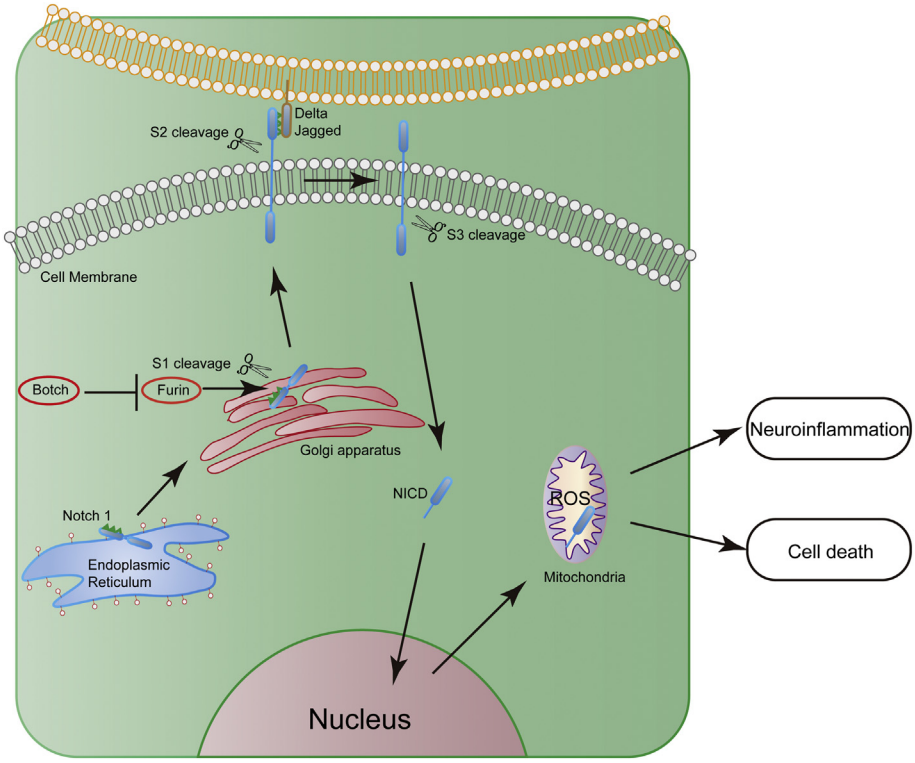

Fig. 7. Schematic representations of potential mechanisms of Botch actions in ischemia-reperfusion (I/R) injury.
Ischemic stroke up-regulates the expression of Botch. Botch antagonizes the maturation of Notch1 by inhibiting the S1 furin-like cleavage of Notch1. Decreasing NICD mitochondria translocation reduces the accumulation of oxidizing substances in cells, which subsequently alleviates neuroinflammation and neuronal cell death.

activation inhibited by siRNA demonstrate worse neurological deficits, lager infarction volume, more neuronal cell death and higher level of neuroinflammation. While Botch overexpression group present less neuronal damage after MCAO/R. In the canonical signaling pathway of Notch in the central nervous system (CNS), the ligand-dependent cleavage of Notch1 eventually promote the release of the Notch intracellular domain (NICD) from the plasma membrane. NICD translocate to the nucleus, which results in the expression of Botch target genes (Pierfelice et al., 2011). Previous studies reveal that Botch is an endogenous Notch inhibitor (Chi et al., 2014; Chi et al., 2012b). Notch signaling is impaired in the presence of Botch via inhibition of furin-like cleavage processing of Notch through deglycinating Notch. The CNS has the ability to activate profound neuroprotection in response to sublethal insults. Dai et al. performed a functional clonal screening of mouse cortical neurons treated with ischemic preconditioning and found that Botch is one of the 33 genes that provided neuroprotection against OGD or excitotoxic exposure to *N*-methyl-D-aspartate (NMDA) in primary cortical neurons (Dai et al., 2010). Indirect evidence could the provided by studies that applying chemical inhibition of Notch activation. N-[N-(3, 5-difluorophenacetyl)-L-alanyl]-*S*-phenylglycine tbutyl ester (DAPT) or γ-secretase inhibitor XXI (compound E) can reduce neuronal death and the volume of cerebral infarction after ischemic injury (Cheng et al., 2014; Li et al., 2016b).

Ischemic injury in the brain after stroke causes neuronal cell death and activates microglia-induced neuroinflammatory responses (Alberi et al., 2013; Stonesifer et al., 2017). Damage to cells induces inflammatory cells to generate ROS and inflammatory cytokines (Blaser et al., 2016). Inflammatory factors subsequently activate microglia and generate inflammatory mediators, including matrix metalloproteinases (MMPs), inducible nitric oxide synthase (iNOS), cytokines and more ROS (Lee et al., 2014; Zhang et al., 2017). These pro-inflammatory molecules ultimately result in brain edema and cell death in the infarct core and penumbra (Kim et al., 2014; Masahito and Yenari, 2015). The Notch signaling pathway is a key pathway after ischemic insult, which coordinates NF-κB/p53 signaling to regulate microglial activation and the corresponding inflammatory response (Alberi et al., 2013; Stonesifer et al., 2017). Previous studies also suggest that the Notch signaling pathway mediates inflammatory responses in diseases such as tumors (Fazio et al., 2016; Fazio and Ricciardiello, 2016) and immune diseases (Sheng et al., 2018). In our study, we demonstrated that neuroinflammation and Notch1 signaling were activated after brain ischemia. Botch alleviated microglial activation and prevented the development of neuroinflammation by antagonizing the activation of Notch1 signaling.

Furthermore, there is evidence that Notch1 is involved in inflammatory regulation via mechanisms that involve mitochondria and ROS. Activated Notch signaling has been shown to be recruited into mitochondria and to upregulate mitochondrial oxidative phosphorylation and ROS (mtROS) (Jun et al., 2015). Moreover, Notch1 silencing significantly decreases ROS and inflammatory-cytokine production (Xie et al., 2015). In addition, the activation of Notch signaling plays an important role in cardiac HeLa, HEK-293 and COS-7 cell survival (Perumalsamy et al., 2010), as well as in cardiac differentiation via regulating mitochondria (Atsuko et al., 2013). Similar to the study of Jun et al (Jun et al., 2015), our study found that NICD translocation to mitochondria induced an increase in mitochondrial ROS, which could be reversed by Botch overexpression (as Botch is a known Notch inhibitor).

We acknowledge that our study has several limitations. In order to minimize the variables involved, we used only adult male rats for all experiments. However, stroke clinically occurs most often in both elderly males and females. Future experiments should investigate ischemic stroke in aged rats to better simulate the human condition. Additionally, the relationship between Botch and NICD in mitochondria requires continued studies for its further elucidation. Although Botch has exhibited promising application prospects in preclinical studies, whether it has neuroprotection in clinical applications requires further validation.

5. Conclusion

Our study provided evidence that Botch might be a neuroprotective target in ischemic stroke. Botch reduced microglial-mediated neuroinflammation via inhibiting injury-induced NICD upregulation and

mitochondrial translocation (Fig. 7).

Declaration of Competing Interest

The authors declare that there are no conflicts of interest.

Acknowledgements

This work is supported by grants from National Natural Science Foundation of China (No. 81601011), Natural Science Foundation of Jiangsu Province (No. BK20160345) and Suzhou Government (No. KJXW2016002), and National key R&D Program of China (No. 2017YFC0114300).

References

Alberi, L., Hoey, S.E., Brai, E., Scotti, A.L., Marathe, S., 2013. Notch signaling in the brain: in good and bad times. Ageing Res. Rev. 12, 801–814.

Arumugam, T.V., Chan, S.L., Jo, D.G., Yilmaz, G., Tang, S.C., Cheng, A., Gleichmann, M., Okun, E., Dixit, V.D., Chigurupati, S., Mughal, M.R., Ouyang, X., Miele, L., Magnus, T., Poosala, S., Granger, D.N., Mattson, M.P., 2006. Gamma secretase-mediated Notch signaling worsens brain damage and functional outcome in ischemic stroke. Nat. Med. 12, 621–623.

Atsuko, K., Sara, C., Yun, C., Dorn, G.W., Luca, S., 2013. Mitochondrial fusion directs cardiomyocyte differentiation via calcineurin and Notch signaling. Science 342, 734–737.

Blaser, H., Dostert, C., Mak, T.W., Brenner, D., 2016. TNF and ROS crosstalk in inflammation. Trends Cell Biol. 26, 249–261.

Chen, J., Li, Y., Wang, L., Zhang, Z., Lu, D., Lu, M., Chopp, M., 2001. Therapeutic benefit of intravenous administration of bone marrow stromal cells after cerebral ischemia in rats. Stroke 32, 1005–1011.

Cheng, Y.L., Park, J.-S., Manzanero, S., Choi, Y., Baik, S.-H., Okun, E., Gelderblom, M., Fann, D.Y.-W., Magnus, T., Launikonis, B.S., 2014. Evidence that collaboration between HIF-1α and Notch-1 promotes neuronal cell death in ischemic stroke. Neurobiol. Dis. 62, 286–295.

Chi, Z., Zhang, J., Tokunaga, A., Harraz, M., Byrne, S., Dolinko, A., Xu, J., Blackshaw, S., Gaiano, N., Dawson, T., 2012a. Botch promotes neurogenesis by antagonizing Notch. Dev. Cell 22, 707–720.

Chi, Z., Zhang, J., Tokunaga, A., Harraz, M.M., Byrne, S.T., Dolinko, A., Xu, J., Blackshaw, S., Gaiano, N., Dawson, T.M., Dawson, V.L., 2012b. Botch promotes neurogenesis by antagonizing Notch. Dev. Cell 22, 707–720.

Chi, Z., Byrne, S.T., Dolinko, A., Harraz, M.M., Kim, M.S., Umanah, G., Zhong, J., Chen, R., Zhang, J., Xu, J., Chen, L., Pandey, A., Dawson, T.M., Dawson, V.L., 2014. Botch is a gamma-glutamyl cyclotransferase that deglycinates and antagonizes Notch. Cell Rep. 7, 681–688.

Dai, C., Liang, D., Li, H., Sasaki, M., Dawson, T.M., Dawson, V.L., 2010. Functional identification of neuroprotective molecules. PLoS One 5, e15008.

Dirnagl, U., Iadecola, C., Moskowitz, M.A., 1999. Pathobiology of ischaemic stroke: an integrated view. Trends Neurosci. 22, 391–397.

Fazio, C., Ricciardiello, L., 2016. Inflammation and Notch signaling: a crosstalk with opposite effects on tumorigenesis. Cell Death Dis. 7, e2515.

Fazio, C., Piazzi, G., Vitaglione, P., Fogliano, V., Munarini, A., Prossomariti, A., Milazzo, M., D'Angelo, L., Napolitano, M., Chieco, P., 2016. Inflammation increases NOTCH1 activity via MMP9 and is counteracted by eicosapentaenoic acid-free fatty acid in colon cancer cells. Sci. Rep. 6, 20670.

GBD 2016 Lifetime Risk of Stroke Collaborators, 2018. Global, regional, and country-specific lifetime risks of stroke, 1990 and 2016. N. Engl. J. Med. 379, 2429–2437.

Jun, X., Feng, C., Tongsheng, G., Vasu, P., Lee, W.N.P., French, S.W., Hidekazu, T., 2015. NOTCH reprograms mitochondrial metabolism for proinflammatory macrophage activation. J. Clin. Investig. 125, 1579–1590.

Kim, J.Y., Kawabori, M., Yenari, M.A., 2014. Innate inflammatory responses in stroke: mechanisms and potential therapeutic targets. Curr. Med. Chem. 21.

Lee, E.J., Moon, P.G., Baek, M.C., Kim, H.S., 2014. Comparison of the effects of matrix metalloproteinase inhibitors on TNF-alpha release from activated microglia and TNF-alpha converting enzyme activity. Biomol. Ther. 22, 414–419.

Li, S., Zhang, X., Wang, Y., Du, Y., Liu, H., 2012a. DAPT protects brain against cerebral ischemia by down-regulating the expression of Notch 1 and nuclear factor kappa B in rats. Neurol. Sci. 33, 1257–1264.

Li, S., Zyang, X., Wang, Y., Ji, H., Du, Y., Liu, H., 2012b. DAPT protects brain against cerebral ischemia by down-regulating the expression of Notch 1 and nuclear factor kappaB in rats. Neurological Sciences 33, 1257–1264.

Li, Z., Wang, J., Zhao, C., Ren, K., Xia, Z., Yu, H., Jiang, K., 2016a. Acute blockage of Notch signaling by DAPT induces neuroprotection and neurogenesis in the neonatal rat brain after stroke. Transl. Stroke Res. 7, 132–140.

Li, Z., Wang, J., Zhao, C., Ren, K., Xia, Z., Yu, H., Jiang, K., 2016b. Acute blockage of Notch signaling by DAPT induces neuroprotection and neurogenesis in the neonatal rat brain after stroke. Transl. Stroke Res. 7, 132–140.

Liu, W., Li, R., Yin, J., Guo, S., Chen, Y., Fan, H., Li, G., Li, Z., Li, X., Zhang, X., He, X., Duan, C., 2019. Mesenchymal stem cells alleviate the early brain injury of subarachnoid hemorrhage partly by suppression of Notch1-dependent neuroinflammation: involvement of botch. J. Neuroinflammation 16, 8.

Masahito, K., Yenari, M.A., 2015. Inflammatory responses in brain ischemia. Curr. Med. Chem. 22.

Mei, B., Li, H., Zhu, J., Yang, J., Yang, Z., Wen, Z., Xiang, L., Shen, H., Shen, M., Gang, C., 2017. Neuroprotection of botch in experimental intracerebral hemorrhage in rats. Oncotarget 8, 95346–95360.

Perumalsamy, L.R., Manjula, N., Apurva, S., 2010. Notch-activated signaling cascade interacts with mitochondrial remodeling proteins to regulate cell survival. Proc. Natl. Acad. Sci. U. S. A. 107, 6882–6887.

Pierfelice, T., Alberi, L., Gaiano, N., 2011. Notch in the vertebrate nervous system: an old dog with new tricks. Neuron 69, 840–855.

Powers, W.J., Rabinstein, A.A., Ackerson, T., Adeoye, O.M., Bambakidis, N.C., Becker, K., Biller, J., Brown, M., Demaerschalk, B.M., Hoh, B., 2018. 2018 guidelines for the early Management of Patients with Acute Ischemic Stroke: a guideline for healthcare professionals from the American Heart Association/American Stroke Association. J. Vasc. Surg. 67, 1934.

Shen, H., Liu, C., Zhang, D., Yao, X., Zhang, K., Li, H., Chen, G., 2017. Role for RIP1 in mediating necroptosis in experimental intracerebral hemorrhage model both in vivo and in vitro. Cell Death Dis. 8, e2641.

Sheng, X., Zuo, X., Liu, X., Zhou, Y., Sun, X., 2018. Crosstalk between TLR4 and Notch1 signaling in the IgA nephropathy during inflammatory response. Int. Urol. Nephrol. 50, 779–785.

Stocchetti, N., Taccone, F.S., Citerio, G., Pepe, P.E., Le Roux, P.D., Oddo, M., Polderman, K.H., Stevens, R.D., Barsan, W., Maas, A.I., Meyfroidt, G., Bell, M.J., Silbergleit, R., Vespa, P.M., Faden, A.I., Helbok, R., Tisherman, S., Zanier, E.R., Valenzuela, T., Wendon, J., Menon, D.K., Vincent, J.L., 2015. Neuroprotection in acute brain injury: an up-to-date review. Crit. Care 19, 186.

Stonesifer, C., Corey, S., Ghanekar, S., Diamandis, Z., Acosta, S.A., Borlongan, C.V., 2017. Stem cell therapy for abrogating stroke-induced neuroinflammation and relevant secondary cell death mechanisms. Prog. Neurobiol. 158, 94–131.

Wang, Y., Gao, A., Xu, X., Dang, B., You, W., Li, H., Yu, Z., Chen, G., 2015. The Neuroprotection of lysosomotropic agents in experimental subarachnoid hemorrhage probably involving the apoptosis pathway triggering by cathepsins via chelating intralysosomal iron. Mol. Neurobiol. 52, 64–77.

Wang, Z., Chen, Z., Yang, J., Yang, Z., Yin, J., Zuo, G., Duan, X., Shen, H., Li, H., Chen, G., 2016. Identification of two phosphorylation sites essential for annexin A1 in blood-brain barrier protection after experimental intracerebral hemorrhage in rats. J. Cereb. Blood Flow Metab. 37, 0271678X16669513.

Xie, H., Sun, J., Chen, Y., Zong, M., Li, S., Wang, Y., 2015. EGCG attenuates uric acid-induced inflammatory and oxidative stress responses by medicating the NOTCH pathway. Oxidative Medicine & Cellular Longevity 2015, 1–10.

Yuan, Z.F., Tang, Y.M., Xu, X.J., Li, S.S., Zhang, J.Y., 2016. 10-Hydroxycamptothecin induces apoptosis in human neuroblastoma SMS-KCNR cells through p53, cytochrome c and caspase 3 pathways. Neoplasma 63, 72.

Zhang, L., Chen, J., Li, Y., Zhang, Z.G., Chopp, M., 2000. Quantitative measurement of motor and somatosensory impairments after mild (30 min) and severe (2 h) transient middle cerebral artery occlusion in rats. J. Neurol. Sci. 174, 141–146.

Zhang, Z., Zhang, Z., Lu, H., Yang, Q., Wu, H., Wang, J., 2017. Microglial polarization and inflammatory mediators after intracerebral hemorrhage. Mol. Neurobiol. 54, 1874–1886.

Zhu, J., Liu, Q., Jiang, Y., Wu, L., Xu, G., Liu, X., 2015. Enhanced angiogenesis promoted by human umbilical mesenchymal stem cell transplantation in stroked mouse is Notch1 signaling associated. Neuroscience 288–299 290C.